A boronate-based fluorescent probe for the selective detection of cellular peroxynitrite

ARTICLE *in* CHEMICAL COMMUNICATIONS · JULY 2014

Impact Factor: 6.83 · DOI: 10.1039/c4cc02943g · Source: PubMed

5 AUTHORS, INCLUDING:

Yongdoo Choi
National Cancer Center Korea
53 PUBLICATIONS **1,279** CITATIONS

SEE PROFILE

ChemComm

COMMUNICATION

View Article Online
View Journal | View Issue

A boronate-based fluorescent probe for the selective detection of cellular peroxynitrite†

Cite this: *Chem. Commun.*, 2014, 50, 9353

Received 21st April 2014,
Accepted 21st June 2014

DOI: 10.1039/c4cc02943g

www.rsc.org/chemcomm

Jiyoung Kim,[a] Jeesook Park,[a] Hawon Lee,[b] Yongdoo Choi*[b] and Youngmi Kim*[a]

A boronate-based fluorescent probe 1 for the selective monitoring of intracellular peroxynitrite has been developed. The probe takes advantage of the fast reaction of an arylboronate group with peroxynitrite, yielding a corresponding phenol that undergoes spontaneous subsequent reactions to produce a strongly fluorescent product associated with a large turn-on signal.

Peroxynitrite ($ONOO^-$) in living systems is receiving increasing attention owing to the diverse roles it plays as a highly reactive oxidant and an efficient nitrating agent in many physiological and pathological processes.[1] $ONOO^-$ is formed by the diffusion-controlled reaction between nitric oxide ($^{\bullet}NO$) and superoxide anion ($^{\bullet}O_2^-$) in inflammatory cells such as neutrophils and macrophages.[2] In contrast to its beneficial effects in mechanisms employed by hosts to defend against microbial invasion, excessive generation of $ONOO^-$ could have deleterious effects on a wide array of biomolecules in cells, including lipids, proteins, and nucleic acids, leading to cell apoptosis or necrosis,[3] and has been implicated in the genesis and progression of numerous ailments, such as cardiovascular diseases, circulatory shock, inflammation, cancers, ischemic stroke, reperfusion injury, atherosclerosis, and diabetes.[4]

Despite the importance of $ONOO^-$ in human health and diseases, the complex biological roles played by this species in cellular signaling pathways and various diseases have not yet been fully elucidated. One of the main reasons for this lies in the lack of effective chemical tools to measure dynamic changes in $ONOO^-$ concentrations occurring within localized regions of cells. Owing to their documented sensitivity and utility in many biological studies, small-molecule fluorescent probes offer a promising approach for detecting highly reactive $ONOO^-$ *in vivo*.[5] The most popular fluorescent probes developed for this purpose thus far are based on fluorescein or rhodamine dyes, in which nonfluorescent forms are converted to fluorescent products.[6] Although enabling detection of $ONOO^-$, these probes also respond to other highly reactive oxygen species (hROS) such as the hydroxyl radical ($^{\bullet}OH$) and hypochlorite (OCl^-), often with higher sensitivity, and are extensively auto-oxidized. Recent studies have identified several fluorescent probes for $ONOO^-$ that are based on other chemical transformations including aromatic nitration,[7] ketone oxidation reactions[8] and redox reactions of organoselenium/organotellurium compounds.[9] Such probes displayed a response to $ONOO^-$ with variable degrees of sensitivity, however, some of them suffer from a few limitations such as nonspecific reactivity with other ROS, poor photostability, or low water solubility. In order to have practical applications, next-generation $ONOO^-$ probes need to be easily synthesized, and should possess high analyte selectivity and limited susceptibility to auto-oxidation.

Boronate-containing fluorogenic compounds have been used as the basis of the most effective probes for detecting intracellular H_2O_2.[10] However, the results of recent investigations, utilizing a stopped-flow kinetic technique and HPLC analysis, have demonstrated that arylboronates react with $ONOO^-$ to yield corresponding hydroxyl derivatives nearly six orders of magnitude faster than with H_2O_2.[11] We envisioned that the rapid reactions with $ONOO^-$ would make arylboronates ideal substances for use in $ONOO^-$ specific fluorescent probes. Along these lines, observations made in a recent investigation show that a boronate-containing fluorescent probe based on the blue emissive pyrene fluorophore is more responsive to $ONOO^-$ over other ROS.[12] However, positive fluorescence response of the pyrene–boronate sensor was also seen upon treatment with H_2O_2, ClO^-, or OBr^- for 15 min with an insufficient degree of selectivity (*ca.* 3 : 1 in favor of $ONOO^-$ over H_2O_2, ClO^-, or OBr^-), indicating the need for the development of new $ONOO^-$ selective probes. Below, we describe the design and synthesis of the new

[a] *Department of Chemistry, Institute of Nanosensor and Biotechnology, Dankook University, 152 Jukjeon-ro, Suji-gu, Yongin-si, Gyeonggi-do, 448-701, Korea. E-mail: youngmi@dankook.ac.kr; Fax: +82-31-8005-3148; Tel: +82-31-8005-3156*

[b] *Molecular Imaging & Therapy Branch, National Cancer Center, 323 Ilsan-ro, Goyang-si, Gyeonggi-do 410-769, Korea. E-mail: ydchoi@ncc.re.kr; Fax: +82-31-920-2529; Tel: +82-31-920-2512*

† Electronic supplementary information (ESI) available: Synthetic details, additional spectral data, kinetic study, and experiments using living cells. See DOI: 10.1039/c4cc02943g

boronate-derived probe **1**, and demonstrate its application as a highly sensitive and selective fluorescent probe for the detection of $ONOO^-$ in living cells.

A benzothiazolyl iminocoumarin scaffold, serving as an analogue of a coumarin dye, was employed in the design of the new fluorescent probe for monitoring $ONOO^-$. This selection was guided by the excellent photophysical properties, such as high photostabilities and high fluorescence quantum yields, of members of this family. Moreover, iminocoumarins have excitation and emission wavelengths that are longer than those of the related coumarins, making the former more suitable than the latter for biological applications.[13] The boronate probe **1**, designed using these considerations, contains a phenol moiety masked by a *p*-dihydroxyborylbenzyloxy group. This probe is expected to display a low fluorescence quantum yield in solution, because of fast non-radiative decay of the singlet excited state that is facilitated by free rotation about the C–C double bond of an alkene linker. In addition, we hypothesized that reaction of **1** with $ONOO^-$ would promote oxidative hydrolysis of the arylboronate group to generate the corresponding phenol (see Scheme S3 (ESI†) for the detailed mechanism), which would undergo rapid elimination of *p*-quinomethane to produce phenolate **2b**. Rapid cyclization of **2b** would then generate the highly fluorescent benzothiazolyl iminocoumarin **3** (Scheme 1).

Probe **1** was prepared using the two-step sequence outlined in Scheme S1 (ESI†). Benzothiazolyl iminocoumarin **3**, the expected product resulting from reaction of **1** with $ONOO^-$, was also prepared utilizing a previously described general method.[13]

The photophysical properties of **1** and **3** were evaluated in order to demonstrate that they are compatible with the use of **1** as a turn-on fluorescent probe for $ONOO^-$ (Table S1, Fig. S1 and S2, ESI†). The results show that **1** in ethanol has an absorption maximum at 482 nm and a fluorescence maximum at 536 nm corresponding to weak green emission (Φ_F = 0.01). The absorption and fluorescence emission maxima of **3** in the same solvent occur at 480 nm and 530 nm (Φ_F = 0.96), respectively. In aqueous buffer solution (10 mM phosphate buffer, pH 7.4, 10% ethanol), **1** has an emission maximum at 646 nm (Φ_F = 0.01). This significantly red-shifted emission compared with that in ethanol is attributed to the formation of aggregates in solvents like water, in which **1** has a low solubility. These properties along with the large fluorescence quantum yield (Φ_F) of **3** of 0.62 in aqueous solution clearly demonstrate that **1** could serve as an ideal off–on fluorescent probe for $ONOO^-$.

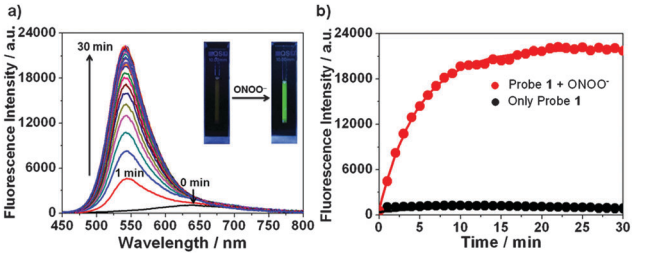

Fig. 1 (a) Time-dependent emission spectra (λ_{ex} = 430 nm) of probe **1** (10 μM) upon treatment with $ONOO^-$ (10 μM) in phosphate buffer (10 mM, pH 7.4, 10% ethanol) at 37 °C. Spectra were recorded every 1 min (0–30 min). Inset: photographs of probe **1** in the absence (left) and presence (right) of $ONOO^-$ after incubation for 30 min at 25 °C under UV light (365 nm) illumination. (b) Change in fluorescence intensity at 540 nm in the presence of $ONOO^-$ (10 μM) as a function of incubation time.

The fluorescence response of **1** toward $ONOO^-$ in aqueous buffer solution (10 mM phosphate buffer, pH 7.4, 10% ethanol) at 37 °C is displayed in Fig. 1. Inspection of the spectra shows that a time-dependent change takes place upon addition of 1 equiv. $ONOO^-$ to the solution of **1** (10 μM). Specifically, over a 0–30 min incubation period (plateaus at 15 min, Fig. 1b), a large blue-shift of the emission spectrum of **1** occurs in concert with a distinct increase in the intensity of emission at 540 nm, which is the emission maximum of **3** (Fig. 1a). At the same time, a significant change in the emission color from pale red to intense green occurs (Fig. 1a, inset). Finally, the fluorescence intensity of **1** does not change under aerated assay conditions when $ONOO^-$ is not present in the solution (Fig. 1b).

HPLC-MS analysis of the mixture generated from the reaction of $ONOO^-$ with **1** confirmed that the fluorescence increase at 540 nm is a consequence of the formation of **3** (Fig. S9, ESI†). The conversion of **1** to **3** is fast (complete within 30 min), and the proposed intermediates, **2a** and **2b**, in the pathway for formation of **3** are not detected by HPLC-MS. These observations show that the new probe **1** should be useful for the detection of $ONOO^-$, which is rapidly metabolised in biological systems.

The response of **1** (10 μM) to different concentrations of $ONOO^-$ in the range of 0–20 μM after incubation times of 30 min was elucidated (Fig. 2a). As expected, the fluorescence intensity at 540 nm increases with increasing $ONOO^-$ concentration within the measured range (Fig. 2a, inset). A good linear relationship exists between the normalized fluorescence intensity at 540 nm (F/F_0) and the concentration of $ONOO^-$ in the concentration range of 3–10 μM (R^2 = 0.998) (Fig. S5, ESI†). The detection limit for $ONOO^-$ using probe **1** was determined on the basis of the signal-to-noise ratio (S/N = 3) to be 2.5 μM, a value that is comparable to those of previously described fluorescent probes for $ONOO^-$. Finally, the concentration dependence of the rise in fluorescence intensity yields a rate constant (k) of **1** to **3** of *ca.* 15 100 M^{-1} min^{-1} for the $ONOO^-$ induced conversion (Fig. S8, ESI†).

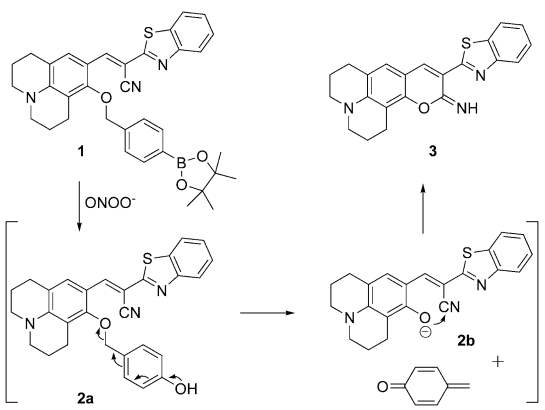

Scheme 1 Chemical structure of **1** and its reaction with $ONOO^-$ to release the fluorescent reporter group **3**.

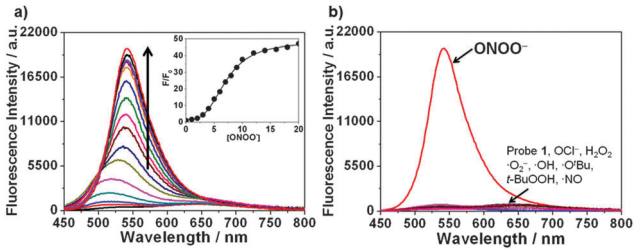

Fig. 2 (a) Fluorescence titration spectra of **1** (10 μM) in the presence of different concentrations of $ONOO^-$. [$ONOO^-$] = 0, 1, 2, 3, 4, 5, 6, 7, 8, 9, 10, 12, 14, 16, 18, 20 μM. Inset shows a plot of the relative fluorescence intensity (F/F_0) at 540 nm as a function of [$ONOO^-$]. (b) Fluorescence emission spectra of **1** (10 μM) in the presence of various ROS (20 μM $ONOO^-$ and 100 μM for other ROS). All spectra were obtained 30 min after addition of each analyte to **1** in phosphate buffer (10 mM, pH 7.4, 10% ethanol) at 37 °C. λ_{ex} = 430 nm.

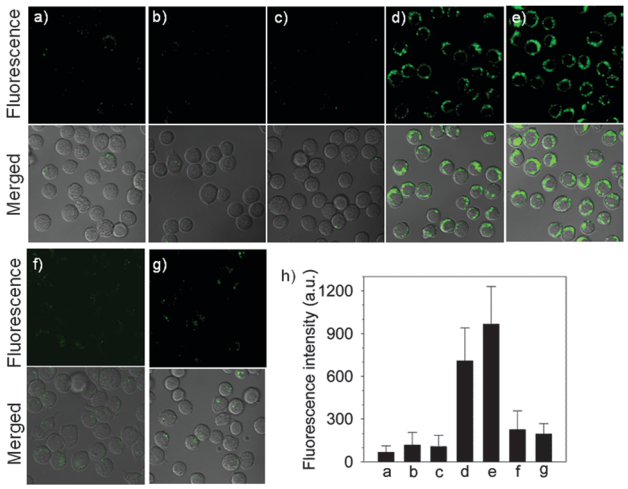

Fig. 3 Confocal fluorescence microscope images of **1** (10 μM)-loaded living macrophage cells (J774A.1) under different conditions. (a) Macrophages were incubated with **1** for 20 min at 37 °C and then imaged; (b) **1**-loaded macrophage cells were incubated with 50 μM H_2O_2 for 30 min; (c) **1**-loaded macrophage cells were incubated with 50 μM NaOCl for 30 min; (d) macrophage cells were co-incubated with SIN-1 (1 mM) and **1** for 20 min; (e) macrophage cells were stimulated with LPS (1 μg mL^{-1}) and IFN-γ (50 ng mL^{-1}) for 4 h, and incubated with **1** for 20 min at 37 °C; (f) NOS inhibitor, AG (5 mM) was co-incubated during LPS/IFN-γ stimulation for 4 h, and incubated with **1** for 20 min at 37 °C; (g) superoxide scavenger, TEMPO (300 μM) was co-incubated during LPS/IFN-γ stimulation for 4 h; the other procedures were the same; (h) graph showing quantification of mean (SD) fluorescence intensity of each cell in a–g correspondingly ($n > 50$). (Upper: fluorescence images, bottom: merged images, Ex = 405 nm, Em = 529–614 nm.)

The selectivity of **1** (10 μM) toward $ONOO^-$ was determined by measuring time-dependent fluorescence changes that take place in the presence of various ROS (20 μM for $ONOO^-$ and 100 μM for hydrogen peroxide H_2O_2, hypochlorite OCl^-, superoxide $^\bullet O_2^-$, hydroxyl radical $^\bullet OH$, *tert*-butoxyl radical $^\bullet O^tBu$, *tert*-butyl hydroperoxide *t*-BuOOH, nitric oxide $^\bullet NO$) in phosphate buffer (10 mM, pH 7.4, 10% ethanol) at 37 °C. As the spectra in Fig. 2b show, only $ONOO^-$ promotes a dramatic enhancement in fluorescence intensity at 540 nm (F/F_0 = 47.1). In contrast, no changes in emission intensities occur when the probe is incubated with other ROS even at higher concentrations. An exception is the case of H_2O_2, which induces a small fluorescence response after 120 min (F/F_0 = 1.6).[14] These results indicate that probe **1** displays a high selectivity *in vitro* for $ONOO^-$ over other ROS. The observations also corroborate the previous finding that boronate-containing small molecules react with $ONOO^-$ much faster than with H_2O_2 or OCl^-.[11]

The potential utility of **1** for the specific imaging of $ONOO^-$ in living cells was evaluated. For this purpose, J774A.1 macrophage cells were incubated with 10 μM **1** for 20 min. After washing with PBS to remove the remaining **1**, the cells were treated with the $ONOO^-$ donor SIN-1 (3-morpholinosydnonimine),[15] which releases equimolar amounts of nitric oxide and superoxide. Confocal microscope images of **1**-loaded macrophages that were treated with SIN-1 show a marked increase in fluorescence intensity arising inside the living cells with a high local concentration in the cytoplasm, whereas the cells that are not treated with SIN-1 show negligible intracellular fluorescence (Fig. 3a and d). In the case of cells treated with 1 mM SIN-1,[16] a more-than 10-fold increase in fluorescence intensity takes place compared to that of **1**-loaded control cells (Fig. 3h). In addition, **1**-loaded macrophages, which are treated with either exogenous H_2O_2 (50 μM) or NaOCl (50 μM) for 30 min, respectively, do not show a noticeable increase in fluorescence intensity (Fig. 3b and c).

Encouraged by its specific response to $ONOO^-$ in living cells, we next determined whether **1** can be employed to image endogenously generated $ONOO^-$ in activated J774A.1 macrophage cells during phagocytosis. Macrophage cells are known to produce ROS at high levels upon physiological stimulation by lipopolysaccharide (LPS), an inducible nitric oxide synthase (iNOS), combined with interferon-γ (IFN-γ).[17] J774A.1 cells were treated with these stimulants (IFN-γ; 50 ng mL^{-1} and LPS; 1 μg mL^{-1}) for 4 h and then incubated with **1** (10 μM) for 20 min. In contrast to cells that are not treated with the stimulants, stimulated cells display a 14.4-fold increase in fluorescence intensity (Fig. 3e and h, $P < 0.001$). Moreover, treatment with the nitric oxide synthase inhibitor aminoguanidine (AG)[18] during stimulation of the cells with IFN-γ/LPS prior to incubation with probe **1** leads to greatly attenuated fluorescence within the cells, in a manner that depends on the concentrations of AG (Fig. 3f and Fig. S13, ESI†). In addition, co-incubation with the superoxide scavenger TEMPO (2,2,6,6-tetramethylpiperidine-*N*-oxyl)[18] during stimulation with IFN-γ/LPS leads to a 5-fold decrease in the fluorescence intensity of the cells (Fig. 3g and h, $P < 0.001$), compared with that of **1**-loaded activated macrophage cells (Fig. 3e). The significantly reduced fluorescence signals arising from AG- and TEMPO-treated cells clearly indicate that strong fluorescence from the activated macrophage cells (Fig. 3e) is a consequence of the formation of $ONOO^-$ and its rapid reaction with **1** to form **3**. These results demonstrate that arylboronate probe **1** enables effective detection and visualization of both exogenous and endogenous $ONOO^-$ in living cells.

In summary, we developed an arylboronate-derived fluorescent probe, **1** for monitoring of $ONOO^-$ concentrations in cellular systems, which possesses (1) a fast response, (2) excellent selectivity

and sensitivity toward $ONOO^-$ over other ROS, and (3) a large fluorescence turn-on signal. These features should make **1** a highly effective tool for probing the biological roles of $ONOO^-$ at the cellular level and for exploring diagnostic markers for cellular $ONOO^-$ formation.

This research was supported by a National Research Foundation grant funded by the Korean government (NRF-2013M2B2A4041354 and NRF-2012R1A1A2038694).

Notes and references

1 C. Ducrocq, B. Blanchard, B. Pignatelli and H. Ohshima, *Cell. Mol. Life Sci.*, 1999, **55**, 1068.
2 G. Ferrer-Sueta and R. Radi, *ACS Chem. Biol.*, 2009, **4**, 161.
3 C. Szabó and H. Oshima, *Nitric Oxide*, 1997, **1**, 373.
4 P. Pacher, J. S. Beckman and L. Liaudet, *Physiol. Rev.*, 2007, **87**, 315.
5 X. Chen, X. Tian, I. Shin and J. Yoon, *Chem. Soc. Rev.*, 2011, **40**, 4783.
6 I. Johnson and M. T. Z. Spence, *The Molecular Probes Handbook: A Guide to Fluorescent Probes and Labelling Technologies*, 2010.
7 T. Ueno, Y. Urano, H. Kojima and T. Nagano, *J. Am. Chem. Soc.*, 2006, **128**, 10640.
8 D. Yang, H.-L. Wang, Z.-N. Sun, N.-W. Chung and J.-G. Shen, *J. Am. Chem. Soc.*, 2006, **128**, 6004.
9 F. Yu, P. Li, G. Li, G. Zhao, T. Chu and K. Han, *J. Am. Chem. Soc.*, 2011, **133**, 11030.
10 A. R. Lippert, G. C. Van de Bittner and C. J. Chang, *Acc. Chem. Res.*, 2011, **44**, 793.
11 J. Zielonka, A. Sikora, M. Hardy, J. Joseph, B. P. Dranka and B. Kalyanaraman, *Chem. Res. Toxicol.*, 2012, **25**, 1793.
12 F. Yu, P. Song, P. Li, B. Wang and K. Han, *Analyst*, 2012, **137**, 3740.
13 T.-I. Kim, H. Kim, Y. Choi and Y. Kim, *Chem. Commun.*, 2011, **47**, 9825.
14 The rate constant (k) for the H_2O_2-induced conversion of **1** to **3** was found to be *ca.* 2.24 M^{-1} min^{-1}.
15 N. Ashki, K. C. Hayes and F. Bao, *Neuroscience*, 2008, **156**, 107.
16 N. Kuzkaya, N. Weissmann, D. G. Harrison and S. Dikalov, *Biochem. Pharmacol.*, 2005, **70**, 343.
17 R. B. Lorsbach, W. J. Murphy, C. J. Lowenstein, S. H. Snyder and S. W. Russell, *J. Biol. Chem.*, 1993, **268**, 1908.
18 R. B. R. Muijsers, E. van den Worm, G. Folkerts, C. J. Beukelman, A. S. Koster, D. S. Postma and F. P. Nijkamp, *Br. J. Pharmacol.*, 2000, **130**, 932.

